Available online at www.sciencedirect.com

ScienceDirect

Procedia Computer Science 105 (2017) 183 – 190

Procedia Computer Science

2016 IEEE International Symposium on Robotics and Intelligent Sensors, IRIS 2016, 17-20 December 2016, Tokyo, Japan

The Control of a Lower Limb Exoskeleton for Gait Rehabilitation: A Hybrid Active Force Control Approach

A. P.P. A. Majeed[a]*, Z. Taha[a], A.F.Z. Abidin[b], M. A. Zakaria[a], I. M. Khairuddin[a], M. A. M. Razman and Z. Mohamed[c]

[a]*Innovative Manufacturing, Mechatronics & Sports Laboratory (iMAMS), Faculty of Manufacturing Engineering, Universiti Malaysia Pahang, 26600 Pekan, Pahang, Malaysia*
[b]*Faculty of Electrical Engineering, Universiti Teknologi MARA, 81750 Masai, Johor Malaysia*
[c]*Faculty of Mechanical Engineering, Universiti Teknologi MARA, 40450 Shah Alam Selangor, Malaysia*

Abstract

This paper focuses on the modelling and control of a three-link lower limb exoskeleton for gait rehabilitation. The exoskeleton that is restricted to the sagittal plane is modelled together with a human lower limb model. In this case study, a harmonic disturbance is excited at the joints of the exoskeleton whilst it is carrying out a joint space trajectory tracking. The disturbance is introduced to examine the compensating efficacy of the proposed controller. A particle swarm optimised active force control strategy is proposed to augment the disturbance regulation of a conventional proportional-derivative (PD) control law. The simulation study suggests that the proposed control approach mitigates well the disturbance effect whilst maintaining its tracking performance which is seemingly in stark contrast with its traditional PD counterpart.

Peer-review under responsibility of organizing committee of the 2016 IEEE International Symposium on Robotics and Intelligent Sensors(IRIS 2016).

Keywords: active force control; particle swarm optimisation; three-link manipulator; robust, gait rehabilitation; trajectory tracking control.

* Corresponding author. Tel.: +609 424 6358; fax: +609 424 5888.
E-mail address: anwarmajeed@imamslab.com

Peer-review under responsibility of organizing committee of the 2016 IEEE International Symposium on Robotics and Intelligent Sensors(IRIS 2016).
doi:10.1016/j.procs.2017.01.204

1. Introduction

Approximately 8% of Malaysia's population is well over 60 years old.[1,2] It has also been reported in the Malaysian Ministry of Health's annual report 2011 that about 11% and 7.2% of children aged between 0 to 18 years were discovered with physical and cerebral palsy disabilities, respectively.[2,3] The report further opines that there is an average of threefold increase in the number of stroke patients in addition to 1.2 million new diabetic cases recorded per annum. More often than not, gait disorders affect the abovementioned percentile.[4] Gait is essentially the capability of a person in keeping balance and assume the upright position as well as one's ability in starting and maintaining rhythmic stepping.[5] This form of disorder may originate from cerebellar disease, stroke, neuromuscular disease, cardiac disease, cognitive impairment, spinal or brain injury amongst others.[6,7]

Due to the growing of ageing society worldwide aside from other contributing factors, the requirement for such rehabilitation services is on the rise.[1–3,6,7] Traditional rehabilitation therapy often requires the support of at least two physical therapists, nevertheless, this form of therapy is deemed too laborious to the therapist as well as cost demanding.[8] This scenario has led the research community as a whole to mitigate the shortcomings of traditional rehabilitation therapy in addition to the increasing demand for gait rehabilitation through robotics. The control strategies that have been reported in the literature may be demarcated into four main classes, namely, bio-signal based control, position tracking control, force and impedance control as well as adaptive control.[9]

It is evident from the literature that the impaired limb's mobility may be enhanced over continuous and repetitive training.[10,11] This method of training is non-trivial in particular the early phase of rehabilitation through which passive mode is essential. This form of treatment may be accomplished through positional or joint based trajectory tracking control. This study intends to investigate the tracking performance of a simple yet robust control scheme viz. a hybrid proportional-derivative (PD) particle swarm optimised active force control (PSOAFC) of a three DOF lower limb exoskeleton system subjected to a form of disturbance. The system is aimed to rehabilitate the flexion/extension of the hip, knee, and ankle, respectively. The performance of the proposed control architecture shall then be compared to a standard PD controller by considering the same operating conditions of the former.

2. Lower Limb Dynamics

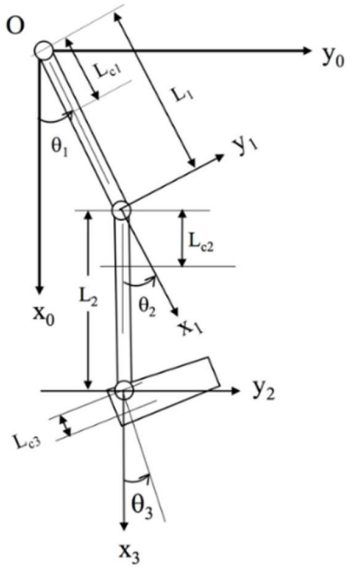

Fig. 1. Three link manipulator model resembling human lower limb (After[12])

The lower limb dynamics of the human limb and exoskeleton are modelled as rigid links joined by joints (bones) as depicted in Fig. 1. The model is restricted to the sagittal plane whilst the human-machine interaction is assumed to be seamless and free from frictional elements. In Figure 1 the subscripts 1, 2 and 3 illustrates the parameters of the first link (thigh), second link (crus/shank) and third link (foot) respectively, as well as the position of the hip, knee and ankle joints respectively. L is the length segments of the limb; L_c is the length segments of the limb about its centroidal axis and θ is the angular position of the links. The Euler-Lagrange formulation is used to derive the governing equations for the nonlinear dynamic system as below[13]

$$\boldsymbol{\tau} = \mathbf{D}(\theta)\ddot{\theta} + \mathbf{C}(\theta,\dot{\theta}) + \mathbf{G}(\theta) + \boldsymbol{\tau}_{\mathbf{d}} \tag{0}$$

where $\boldsymbol{\tau}$ is the actuated torque vector, **D** is the 3 × 3 inertia matrix of the system, **C** is the centripetal and Coriolis torque vector, **G** is the gravitational torque vector, whilst $\boldsymbol{\tau}_{\mathbf{d}}$ is the external disturbance torque vector. In the study, the mass, m and the mass moment of inertia, I of the exoskeleton as well as the limbs are coupled together, and the gravitational constant considered is 9.81 m/s^2. The human lower limb parameters were obtained through the anthropometric parameter of human segments.[12] The total mass is taken as 56.7 kg. Other relevant parameters are listed in section 5.

3. Control Architecture

The thesis of AFC was initially formulated by Hewit and Burdess.[14] Mailah et al. have extended the efficacy of the control law through integrating intelligent methods in approximating the inertial matrix of the dynamic system that in turn triggers the disturbance rejection response of the controller.[15–21] Moreover, the robustness of the method has been demonstrated in a number of different applications both numerically as well as experimentally.[14-21] A schematic of the PSOAFC scheme with the PD component employed to the exoskeleton is shown in Fig. 2.

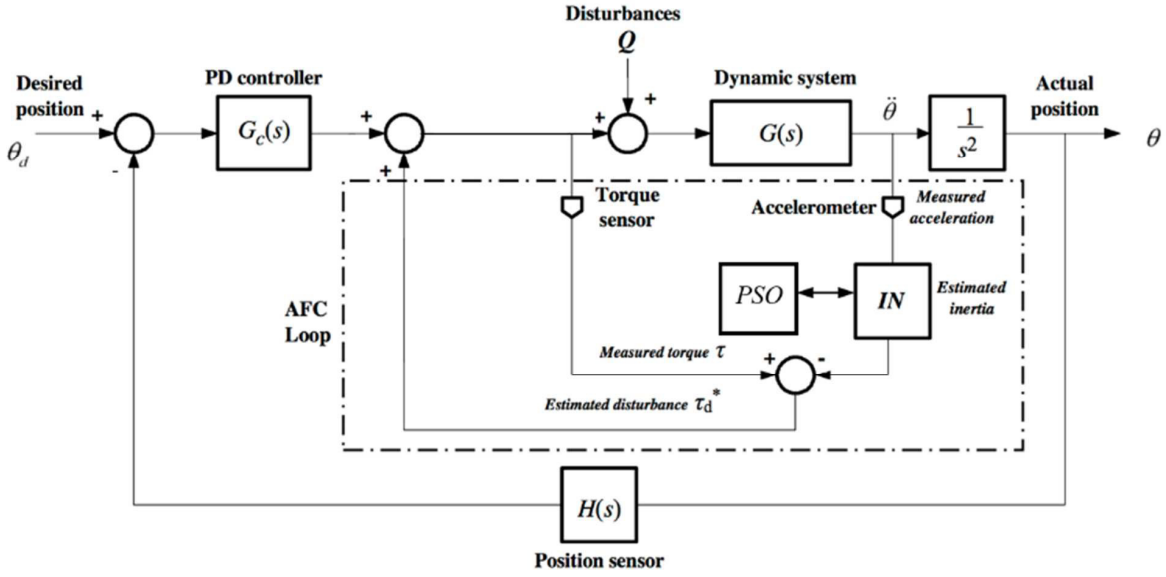

Fig. 2. PD with PSOAFC scheme for the control of the lower limb exoskeleton

The torque generated is driven by the conventional PD control law; that may be expressed as[17]

$$\tau = P(\theta_{\mathrm{d}} - \theta) + D(\dot{\theta}_{\mathrm{d}} - \dot{\theta}) \tag{2}$$

where, θ_{d} and θ are the desired and current angular positions, respectively, $\dot{\theta}_{\mathrm{d}}$ and $\dot{\theta}$ are the derivative (angular velocities) of the aforementioned parameters, respectively. P and D are the derivative and proportional gains, respectively. In this study, the aforementioned gains were properly tuned heuristically. In order to remove the actual disturbances τ_{d}, the estimated disturbance torque τ_{d}^{*} has to be computed and is expressed via

$$\tau_{\mathrm{d}}^{*} = \tau - \mathbf{IN}\ddot{\theta} \tag{3}$$

where **IN** is the approximated inertial matrix, $\ddot{\theta}$ is the measured acceleration signal, whilst τ is the measured applied control torque. **IN** may be represented through

$$[\mathbf{IN}] = [\mathbf{D}] \tag{4}$$

where only the diagonal terms of **D** are considered. The off-diagonal matrix terms may be ignored.[14] The acceleration, as well as the actuated torque of the lower limbs, were also assumed to be perfectly modelled (noise are ignored) in the study. Nonetheless, it is important at this juncture to note that effective disturbance compensation effect of the AFC loop is only triggered if a judicious estimated inertia matrix is attained. In this study, the acquisition of the estimated inertial matrix is obtained through particle swarm optimisation (PSO).

PSO is a robust stochastic optimisation technique inspired by the behaviour of a bird flock by Kennedy and Eberhart.[22] PSO has been employed over a wide range of applications, primarily due to its robustness and its limited number of parameters adjustments.[23-27] Each particle in a swarm will include the position (s) as well as its velocity (v) of the particles.

$$s_i^{k+1} = s_i^k + v_i^{k+1} \tag{5}$$

$$v_i^{k+1} = \omega v_i^k + c_1 r_1 \left(pbest_i - s_i^k \right) + c_2 r_2 \left(gbest_i - s_i^k \right) \tag{6}$$

Referring to (5) and (6), s_i^{k+1} and v_i^{k+1} are the next particle position and velocity whilst v_i^k and s_i^k are the particle i's velocity and position at the k-th generation. r_1 and r_2 are random numbers to induce the stochastic nature of the particles, whilst the cognitive and social coefficients viz. c_1 and c_2 that influences the velocity of the particles are both taken as 1.42 in this study. The personal best (pbest) is the best solution found by each particle in a swarm whilst the global best (gbest) is the best solution amongst the pbest. The gbest and pbest position updates the velocity of the particle through (6). There are various types of dynamic adjustment strategies for the inertia weight, however, in this study the linearly decreasing inertia weight, ω is utilised

$$\omega = \omega_{\max} - \left(\frac{\omega_{\max} - \omega_{\min}}{k_{\max}} \right) * k \tag{7}$$

where the maximum and minimum value of the inertia weight i.e. $\omega_{\max}$ and $\omega_{\min}$ are selected as 0.9 and 0.4 respectively as it has been reported in the literature that the adopted values are able to provide excellent results for a

myriad of real world applications. k and k_{max} are the particle at k-th generation and its maximum generation, respectively. The performance index employed in this study is the minimisation of the sum of the root mean square error (RMSE) in which PSO is implemented to judiciously approximate a set of suitable **IN** value governed by the track error information.

4. Simulation

The simulation study was performed by utilising MATLAB and Simulink software packages. The simulation parameters employed in the study are:

Lower limb parameters (human combined with exoskeleton):

Limb lengths: $L_1 = 0.314$ m, $L_2 = 0.425$ m, L_3=0.425 m;
Centre of mass:
$L_{c1} = 0.1360$ m, $L_{c2} = 0.1840$ m, L_{c3}= 0.0244.m;
Limb masses: $m_1 = 5.67$ kg, $m_2 = 2.64$ kg, $m_3 = 0.82$ kg;
Mass moment of inertia:
$I_1 = 0.0583$ kg.m^2, $I_2 = 0.0434$ kg.m^2, I_3=0.028 kg.m^2;

Controller parameters:
Classical PD
The proportional (P) and derivative (D) gains:
$P_1 = 4\,000$, $D_1 = 200$;
$P_2 = 1\,000$, $D_2 = 100$;
$P_3 = 500$, $D_3 = 1.5$;
Proposed PD-PSOAFC
The controller gains employed in the PD-PSOAFC are the same as the classical PD
PSO parameters:
The diagonal elements of estimated inertia matrix range:

$0 \leq \mathbf{IN}_1 \leq 0.5$ kg.m^2 $0 \leq \mathbf{IN}_2 \leq 0.05$ kg.m^2 $0 \leq \mathbf{IN}_3 \leq 0.005$ kg.m^2

Swarm size: 20
Number of iteration: 200
Fitness function:

$$RMSE = \sqrt{\frac{1}{N}\sum_{i=1}^{N} e^2} \tag{8}$$

The lower limb model is prescribed to accomplish a joint space trajectory tracking of a predefined maximum range of motion for 10 seconds at each joint i.e. hip, knee and ankle at 72.5^o, 62.5^o, and 32.5^o respectively[13].

5. Results and Discussion

To ensure the suitable **IN** values are attained, successive trials were executed by the PSO algorithm in minimising the fitness function defined. The swarm size was varied from 5 to 20 with an accrual of 5 particles, whilst the number of iteration was increased from 50 to 200 with an increase of 50 iterations for each swarm size. The optimised values acquired for IN_1, IN_2 and IN_3 are 0.1512 kg.m^2, 0.0034 kg.m^2 and 0.0029 kg.m^2 respectively. Fig. 3 illustrates the convergence rate of the aforementioned optimised parameters.

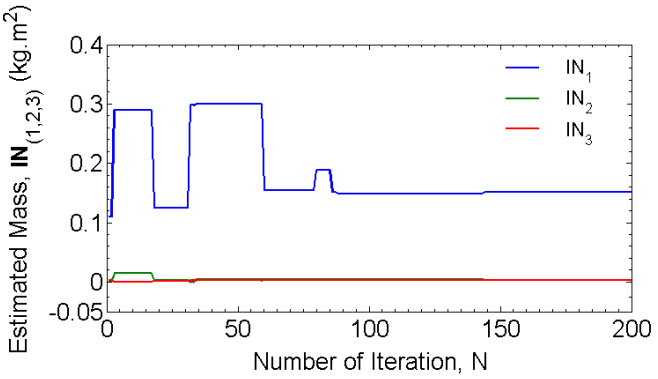

Fig. 3. The estimated inertial parameters of the respective actuated joints by the PSO algorithm.

Figs. 4 (a) to 4 (c) depict the trajectory tracking performance of both the traditional PD as well as PD-PSOAFC algorithms upon the excitation of a harmonic disturbance with an amplitude of 100 N.m. and a frequency of 50 rad/sec applied to each joint respectively (hip, knee, and ankle). Table 1 lists the root mean square (RMS) tracking performance error of individual joint with and without the presence of the aforementioned form of disturbance.

Table 1. Trajectory performance summary.

	Hip joint, θ_1 $error_{RMS}$ (mrad)		Knee joint, θ_2 $error_{RMS}$ (mrad)		Ankle joint, θ_3 $error_{RMS}$ (mrad)	
Disturbance Type	PD	PD-PSOAFC	PD	PD-PSOAFC	PD	PD-PSOAFC
None	6.942	0.137	0.880	1.729	0.229	0.994
Harmonic	40.872	0.142	34.226	1.731	116.685	0.717

It is apparent that from Table 1, the accumulated RMS error of the PD-PSOAFC is 2.86 mrad whereas the PD scheme acquired an accumulated RMS error of 8.051 mrad. It is also noticeable from Table 1 that the respective tracking error of the ankle and knee joints of the latter control scheme is more superior as compared to the former. However, it is worth to note that the error is somewhat allowable in view of the actual trajectory magnitude. Figs. 4 (a) to 4 (c) depicts the performance of the both control scheme upon the introduction of a harmonic disturbance on the respective joints. It is evident that the PSOAFC-based scheme performs reasonably well in regulating the disturbance whilst preserving satisfactory tracking performance in comparison to the classical control law. The accumulated RMS error by the proposed scheme was found to be 2.59 mrad, whilst the RMS error sum of the PD scheme was found to be 191.783 mrad. Based on the simulation study presented, it is without doubt that the proposed control scheme is relatively robust.

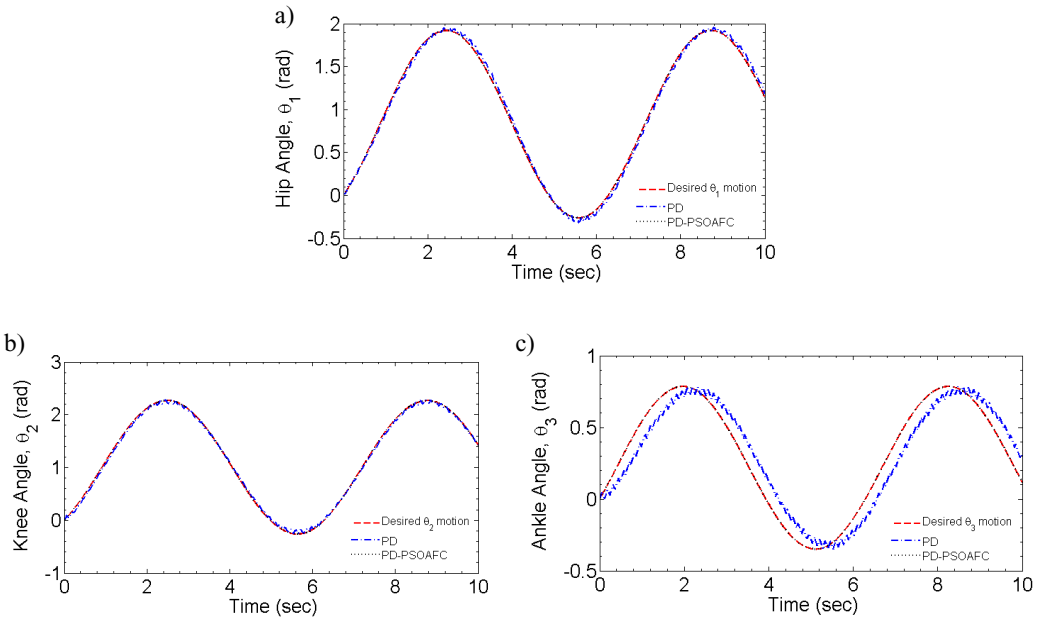

Fig. 4 Trajectory tracking with the inclusion of a harmonic disturbance at the (a) hip joint; (b) knee joint and (c) ankle joint

6. Conclusions

The simulation study provided considerable insight on the effectiveness of the proposed control scheme i.e. PD-PSOAFC in regulating disturbances as compared to the classical PD control scheme. Although the PD control scheme is able to deliver acceptable tracking performance, however, it was demonstrated that upon the introduction of disturbance, its efficacy deteriorates. The superior joint tracking performance accomplished by the PD-PSOAFC, further suggest its relevance in the initial phase of gait therapy. The study could be further extended by considering different types of disturbances as well as other operating conditions.

Acknowledgements

The authors would like to thank Universiti Malaysia Pahang for funding the present study through RDU160343.

References

1. World Health Organization. *World Health Statistics 2014*, http://scholar.google.com/scholar?hl=en&btnG=Search&q=intitle:No+Title#0 (2014).
2. Taha Z, Majeed APPA, Tze MYWP, et al. Preliminary Investigation on the Development of a Lower Extremity Exoskeleton for Gait Rehabilitation: A Clinical Consideration. *J Med Bioeng Vol* 2015; 4.
3. Ministry of Health Malaysia HICPD. Health Facts 2013. *Health Facts* 2013; 22.
4. Sudarsky L, Ronthal M. Gait disorders among elderly patients: a survey study of 50 patients. *Arch Neurol* 1983; **40**: 740–743.
5. Nutt JG, Marsden CD, Thompson PD. Human walking and higher-level gait disorders, particularly in the elderly. *Neurology* 1993; **43**: 268.
6. Franch O, Calandre L, Álvarez-Linera J, et al. Gait disorders of unknown cause in the elderly: Clinical and MRI findings. *J Neurol Sci* 2009; **280**: 84–86.

7. Murray S, Goldfarb M. Towards the use of a lower limb exoskeleton for locomotion assistance in individuals with neuromuscular locomotor deficits. In: *Engineering in Medicine and Biology Society (EMBC), 2012 Annual International Conference of the IEEE*. IEEE, 2012, pp. 1912–1915.
8. Ferris DP, Gordon KE, Beres-Jones JA, et al. Muscle activation during unilateral stepping occurs in the nonstepping limb of humans with clinically complete spinal cord injury. *Spinal Cord* 2004; **42**: 14–23.
9. Meng W, Liu Q, Zhou Z, et al. Recent development of mechanisms and control strategies for robot-assisted lower limb rehabilitation. *Mechatronics*, http://linkinghub.elsevier.com/retrieve/pii/S0957415815000501 (2015).
10. Dietz V, Harkema SJ. Locomotor activity in spinal cord-injured persons. *J Appl Physiol* 2004; **96**: 1954–1960.
11. Wernig A, Müller S, Nanassy A, et al. Laufband therapy based on 'rules of spinal locomotion' is effective in spinal cord injured persons. *Eur J Neurosci* 1995; **7**: 823–829.
12. Winter D a. *Biomechanics and Motor Control of Human Movement*, http://doi.wiley.com/10.1002/9780470549148 (1990).
13. Craig JJ. *Introduction to robotics: mechanics and control*. Pearson Prentice Hall Upper Saddle River, 2005.
14. Hewit J., Burdess J. Fast dynamic decoupled control for robotics, using active force control. *Mech Mach Theory* 1981; **16**: 535–542.
15. Mailah M, Hooi HM, Kazi S, et al. Practical active force control with iterative learning scheme applied to a pneumatic artificial muscle actuated robotic arm. *Int J Mech* 2012; **6**: 88–96.
16. Mailah M, Jahanabadi H, Zain MZM, et al. Modelling and control of a human-like arm incorporating muscle models. *Proc Inst Mech Eng Part C J Mech Eng Sci*; **223**: 1569–1577, http://pic.sagepub.com/content/223/7/1569.abstract (2009, accessed 11 June 2015).
17. Mailah M, Hewit JR, Meeran S. Active force control applied to a rigid robot arm. *J Mek* 1996; **2**: 52–68.
18. Isa WH, Taha Z, Khairuddin IM, et.al. An intelligent active force control algorithm to control an upper extremity exoskeleton for motor recovery. In: *IOP Conference Series: Materials Science and Engineering* 2016; **114**. http://doi:10.1088/1757-899X/114/1/012136
19. Noshadi a., Mailah M. Active disturbance rejection control of a parallel manipulator with self learning algorithm for a pulsating trajectory tracking task. *Sci Iran*; **19**: 132–141, http://dx.doi.org/10.1016/j.scient.2011.11.040 (2012).
20. Priyandoko G, Mailah M, Jamaluddin H. Vehicle active suspension system using skyhook adaptive neuro active force control. *Mech Syst Signal Process* 2009; **23**: 855–868.
21. Kwek LC, Wong EK, Loo CK, et al. Application of active force control and iterative learning in a 5-link biped robot. *J Intell Robot Syst* 2003; **37**: 143–162.
22. Eberhart RC, Kennedy J. A new optimizer using particle swarm theory. In: *Proceedings of the sixth international symposium on micro machine and human science*. New York, NY, 1995, pp. 39–43.
23. Khassetarash A, Hassannejad R. Towards optimal design of sport footwear based on muscle activity and minimum loading rate using simplified model. *Proc Inst Mech Eng Part H J Eng Med* 2015; **229**: 537–548.
24. Bahgaat NK, El-Sayed MI, Hassan MAM, et al. Load Frequency Control in Power System via Improving PID Controller Based on Particle Swarm Optimization and ANFIS Techniques. *Res Methods Concepts, Methodol Tools, Appl Concepts, Methodol Tools, Appl* 2015; 462.
25. Hamza MF, Yap HJ, Choudhury IA. Genetic algorithm and particle swarm optimization based cascade interval type 2 fuzzy PD controller for rotary inverted pendulum system. *Math Probl Eng* 2015; 2015.
26. Zhang S, Lee CKM, Chan HK, et al. Swarm intelligence applied in green logistics: A literature review. *Eng Appl Artif Intell* 2015; **37**: 154–169.
27. Chen S, Arsenault M, Moglo K. Design of a mechanism to simulate the quasi-static moment-deflection behaviour of the osteoligamentous structure of the C3-C4 cervical spine segment in the flexion-extension and lateral bending directions. *Proc Inst Mech Eng H*; **226**: 817–826.